Journal of New Results in Science
dergipark.org.tr/en/pub/jnrs
Open Access

ISSN: 1304-7981 14 (2) (2025) 166-180 doi.org/10.54187/jnrs.1698629

Green Synthesis of Zinc Oxide Nanoparticles from *Malus domestica*, *Tilia cordata*, and its Biological Activities

Nilgün Güler[1], Halime Güzin Aslan[2], Ercan Karaköse[3], Mithat Güllü[4]

Article Info
Received: 17 May 2025
Accepted: 25 Aug 2025
Published: 31 Aug 2025
Research Article

Abstract − This study aimed to evaluate the anticancer and antibacterial drug status of biomass, including zinc oxide (ZnO) nanoparticles (NPs) synthesized from two plant extracts according to the results of Topoisomerase-I enzyme inhibition, DNA cleavage, DNA binding, and antibacterial activity tests. The *Malus domestica* (apple) and *Tilia cordata* (linden) plants were dried and powdered, and their extracts were prepared in pure water. X-Ray Diffraction (XRD), Scanning Electron Microscopy (SEM), and Fourier Transform Infrared (FTIR) analyses were applied for the characterization of the light-yellow powder ZnO NPs. Additionally, Topoisomerase-I enzyme inhibition, DNA cleavage, and DNA binding analyses were performed by agarose gel electrophoresis method. Powder ZnO NPs (biomass) were analyzed by the agar well diffusion method by using two gram-positive and two gram-negative bacteria. According to the XRD analysis results, the peaks obtained show that there is no foreign matter or secondary diffraction peak other than the hexagonal ZnO structure. It was observed that ZnO NPs from *Tilia cordata* extract are effective against *Klebsiella pneumoniae*. ZnO NPs from *Malus domestica* extract have the potential to be an effective human Topoisomerase-I enzyme inhibitor. There was poor DNA cleavage activity in all samples. In ZnO NPs from linden extract, there was an interaction at a 1mg/mL concentration of CT-DNA.

Keywords − *Enzyme inhibition, green synthesis, inorganic drug, anti-bacterial activity, ZnO NPs*

1. Introduction

Nanoparticles are particles that range in size from 1 to 100 nm. Due to their small size and large surface area, they exhibit unique properties such as enhanced catalytic reactivity, biological activity, thermal conductivity, nonlinear optical performance, and chemical stability. As a result, nanoparticles are widely applied in various fields, including healthcare, food, feed, aviation, chemistry, cosmetics, and agriculture [1-3].

Nanoparticles can be synthesized using either physical or chemical methods. Physical processes are often lengthy and difficult to carry out, whereas chemical processes typically involve reagents and procedures that may be harmful to the environment. To overcome these limitations, alternative approaches such as green synthesis have been developed. This environmentally friendly method, which relies on biomaterials, is also referred to as green chemistry and has gained increasing attention in recent years.

There are several studies in the literature on nano ZnO synthesized through green methods. The ability of organisms and organic compounds to reduce metal ions and stabilize them as nanoparticles (NPs) forms the

[1]nilgunkusculu@kayseri.edu.tr (Corresponding Author); [2]guzina@erciyes.edu.tr; [3]ekarakose@kayseri.edu.tr; [4]mgullu@erciyes.edu.tr
[1]Department of Chemistry Technology, Mustafa Çıkrıkçıoğlu Vocational School, Kayseri University, Kayseri, Türkiye
[2]Department of Chemistry, Faculty of Science, Erciyes University, Kayseri, Türkiye
[3]Department of Basic Sciences, Faculty of Engineering, Kayseri University, Kayseri, Türkiye
[4]Department of Biology, Faculty of Science, Erciyes University, Kayseri, Türkiye

basis of green synthesis. In particular, secondary metabolites present in plant extracts, such as flavonoids and other phytochemicals, play a key role in the reduction process [4,5]. For example, a study reported the synthesis of ZnO NPs using extracts derived from Hibiscus leaves [6]. This work is noteworthy as it represents an initial step toward the treatment of diabetes mellitus, one of the most common diseases of our time.

In the literature, the majority of green synthesis research has focused on the preparation of NPs containing silver and gold, as well as the evaluation of their biological activities [7–14]. In addition, studies have also explored the synthesis of NPs containing copper, palladium, and platinum using plant extracts through green synthesis methods [15–19].

There are also publications investigating the antioxidant, antifungal, antibacterial, photodegradative, and cytotoxic properties of ZnO NPs synthesized via green methods [20–26]. In addition, studies in the literature have reported nanosynthesis of the quercetin–iron complex as well as various complexes of copper (II) [27,28]. In some cases, High-Performance Liquid Chromatography–Fourier Transform Infrared Spectroscopy (HPLC–FTIR) analyses were performed to identify which phytochemical secondary metabolites, such as flavonoids, tannins, saponins, and terpenoids, acted as reducing agents in the extracts [29,30].

The co-conjugation of these nanoparticles with secondary metabolites further expands their applicability in industrial biotechnology. Nanoparticle-mediated delivery of therapeutically important flavonoids and other biomolecules can enhance their pharmacological efficacy. For instance, hesperetin-conjugated gold NPs have been explored as a potential drug delivery system to reduce the dosage of chemotherapeutic agents, thereby improving the treatment of hepatocellular carcinoma while minimizing adverse side effects [31].

More recently, several reports have highlighted the potential risks of NPs to both human health and the environment. This underscores the need for reliable detection methods in food and biological samples. A standardized, rapid, and straightforward flavonoid-assisted green synthesis method has been developed for the extraction and detection of Titanium dioxide nanoparticles (TiO2 NPs) from food samples [32]. Moreover, this method can be extended to detect flavonoid residues in biological samples, such as urine and blood [33].

Given its efficiency, low cost, and eco-friendly characteristics, green synthesis represents an important alternative to conventional nanoparticle production methods. To date, NPs have been synthesized from a variety of metal ions using numerous plant extracts; however, ZnO NPs derived from apple and linden extracts have not yet been reported. In the present study, we focused on the interaction of ZnO NPs produced via this method with biomolecules, owing to their environmentally friendly and non-toxic nature. Specifically, this work aimed to investigate the binding of ZnO NPs with DNA molecules, their potential to induce separation within the DNA helix, their interaction with the replication enzyme Topoisomerase-I, and their antibacterial activity. To date, although numerous plant extracts have been employed for the synthesis of zinc oxide nanoparticles (ZnO NPs), no reports exist on the use of apple or linden. The present study aims to investigate the biological interactions of ZnO NPs synthesized by green methods from these sources, with a particular focus on DNA binding, cleavage activity, Topoisomerase-I inhibition, and antibacterial properties.

2. Materials

Plant materials were obtained from local vendors in the Yahyalı district and the Kayseri city center. Apple (S1) and linden (S2) were selected as sources for the green synthesis of ZnO NPs. Zinc nitrate hexahydrate ($Zn(NO3)_2 \cdot 6H_2O$) (Sigma-Aldrich) was employed as the zinc precursor in the synthesis process.

3. Methods

3.1. Preparation of Extracts from Plants

The process began with the cleaning and crushing of apples and linden to obtain their extracts. For each plant, 25 g of material was used and mixed with 100 mL of distilled H2O using a magnetic stirrer for 1 hour at 95 °C. The resulting extract was then cooled to 25 °C and filtered twice through filter paper to remove large particles. The prepared extracts were subsequently stored at 4 °C for use in further experiments [34].

3.2. Green Synthesis of ZnO NPs

The synthesis of zinc oxide nanoparticles was carried out through a simple procedure. Briefly, 5 g of Zn(NO3)2·6H2O and a small amount of distilled water were added to 50 mL of plant extract, and the mixture was magnetically stirred at 100 °C until the ZnO structure was formed. The resulting mixture was then annealed in an oven at 400 °C for 120 minutes, yielding ZnO-NPs in powder form. The light yellow powder thus obtained was used for subsequent biological studies. For characterization, Field Emission Scanning Electron Microscopy (FE-SEM), X-ray Diffraction (XRD), and Fourier Transform Infrared Spectroscopy (FT-IR) analyses were performed on ZnO-NPs synthesized from both plant sources [34].

3.2.1. Explanation of Synthesis Reaction

Figure 1 illustrates the possible reaction pathway for the production of zinc oxide nanoparticles using apple and linden extracts. Volatile phytochemicals such as quercetin-3-glucosides, monomeric and oligomeric compounds, kaempferol, quercetin, cinnamic acid, caffeic acid, rosmarinic acid, and other flavonoid molecules can undergo nucleation with Zn^{2+} ions to form zinc–flavonoid complex molecules. Upon heat treatment (annealing), these complexes are transformed into ZnO-NPs [35].

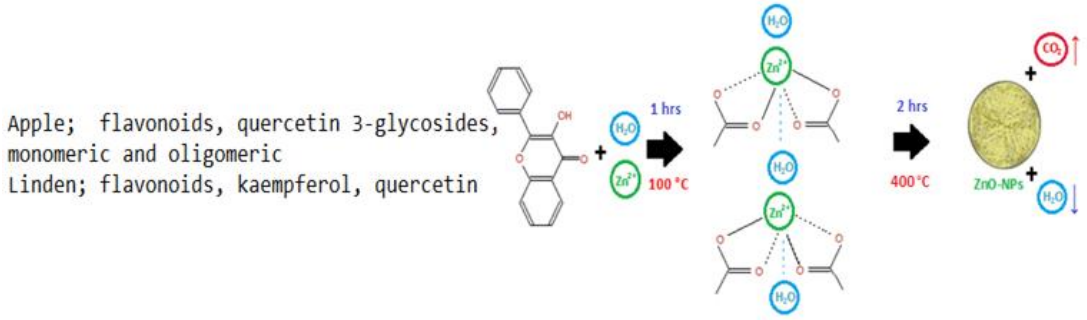


Figure 1. Possible reaction mechanism for ZnO-NPs

However, the proposed reaction mechanism remains unclear and requires further investigation to be fully understood. During the synthesis process, water vapor (H2O(g)) and carbon dioxide (CO2(g)) are released as by-products. Consequently, this ZnO-NP synthesis method is considered environmentally friendly.

3.3. SEM, XRD, and FT-IR Analysis

Structural analyses of zinc oxide nanoparticles were performed using Scanning Electron Microscopy (SEM), X-ray Diffraction (XRD), and Fourier Transform Infrared Spectroscopy (FT-IR). ZnO NPs in dry powder form were directly analyzed with an FEI Quanta SEM, providing image resolutions of up to 1 nm. XRD measurements were carried out on powdered samples using a Panalytical Empyrean diffractometer.

In addition, FT-IR analyses were conducted with a Perkin Elmer Model 400 FT-IR/FT-FIR Spectrometer equipped with a Spotlight 400 Imaging System. This technique was used to determine the presence of

functional groups, evaluate bond characteristics, and identify the binding sites within the structure, as well as to distinguish whether the organic components were aromatic or aliphatic in nature [36].

3.4. Antimicrobial Studies

3.4.1. Microorganism Samples

In this study, four bacterial strains were used to evaluate the antimicrobial activity of zinc oxide nanoparticles synthesized from extracts of two different plant sources. The names of the microorganisms and their corresponding culture collection codes are presented in Table 1.

Table 1. Organism names and culture code

Microorganisms	Organism Code
Bacillus cereus	NRLL B-3008
Escherichia coli	ATCC 25922
Klebsiella pneumonia	ATCC 13883
Staphylococcus epidermidis	ATCC 12228

- *Bacillus cereus:* It is a gram-positive, rod-shaped, endospore-forming, facultative aerobic bacterium, 1x3-4 μm in size. Bacillus cereus, a soil bacterium, can cause food poisoning by affecting many types of food by secreting emetic and enterotoxin [37].
- *Escherichia coli:* It is a gram-negative bacillus with an average length of 2-6 μm and a width of 1-1.5 μm. It is mobile thanks to its peritrich cilia. There are also sleeping species. Some strains have capsules or microcapsules. They do not form spores and are facultative anaerobes [38].
- *Klebsiella pneumonia:* It is a gram-negative bacterium that can cause many diseases. Pneumonia, blood infections, wound or surgical site infections, and meningitis are some of these diseases [39].
- *Staphylococcus epidermidis:* Staphylococcus epidermidis is a type of bacteria among the staphylococci whose seeds are found in clusters. It is gram-positive, catalase-positive, and coagulase-negative. It is naturally found in the person's upper respiratory tract. They are resistant to a wide range of antibiotics, including penicillin and methicillin [40].

3.4.2. Culture Medium Information

- Müller Hinton Agar Medium (gr/lt): 2.0 g meat extract, 17.5 g casein hydrolyzate, 1.5 g starch, 17.0 g agar were all taken into a bottle and sterilized by autoclaving at 121ºC for 15 minutes.
- Müller Hinton Liquid Medium (gr/lt): 2.0 g meat extract, 17.5 g casein hydrolyzate, and 1.5 g starch were all taken into a bottle and sterilized by autoclaving at 121ºC for 15 minutes.

3.4.3. Antimicrobial Activity Study

Antimicrobial activity of the two zinc oxide nanoparticles synthesized from plant extracts was evaluated using the agar well diffusion method. Two Gram-positive and two Gram-negative bacterial strains were employed in the study (Table 1). Bacteria from stock cultures were first grown in Mueller–Hinton broth at 37 °C for 24 hours. Each culture was then reinoculated at 1% (v/v) into fresh broth and incubated for 18 hours until reaching the exponential growth phase. The bacterial suspensions were subsequently adjusted to the standard McFarland density [41].

From each standardized culture, 100 µL was spread onto Mueller–Hinton agar plates using the spread plate technique, after which 6 mm diameter wells were aseptically punched into the agar. A volume of 100 µL of ZnO NPs, dissolved in dimethylformamide (DMF), was introduced into each well, and the plates were incubated under standard conditions. Antimicrobial effects were assessed by measuring the diameters of the inhibition zones around the wells after incubation [42].

3.5. DNA and Enzyme Experiments

3.5.1. Chemicals

Agarose (Isolab), dimethyl sulfoxide (DMSO), double-distilled water (DDW), bromophenol blue, calf thymus deoxyribonucleic acid (CT-DNA), ethylenediaminetetraacetic acid (EDTA), dimethylformamide (DMF), sodium dodecyl sulfate (SDS), Tris base, glycerol, loading dye, ethidium bromide (EtBr), and irinotecan were used in this study. Supercoiled pBR322 plasmid DNA was obtained from Thermo Scientific, while the human topoisomerase I assay kit was purchased from TopoGEN.

3.5.2. DNA Cleavage Experiment

Agarose gel electrophoresis was employed to investigate the effects of zinc oxide (ZnO) nanoparticles synthesized from apple and linden extracts on the double-stranded helical structure of pBR322 plasmid DNA.

3.5.3. DNA Binding Experiment

ZnO NPs obtained from two plants were separately dissolved in dimethylformamide (DMF) to prepare 100 µM stock solutions. Agarose gel electrophoresis was performed to evaluate the interaction of the compounds with calf thymus DNA (CT-DNA). In this study, CT-DNA 2–1 (mg/mL) was prepared in Tris(hydroxymethyl) aminomethane hydrochloride (Tris-HCl) buffer, while the concentrations of the two ZnO NP samples in DMF were fixed at 3% (mg/µL). The mixtures were adjusted to a final volume of 25 µL with buffer in PCR tubes and incubated at 37 °C for 24 hours. After incubation, the samples were loaded onto a 1% agarose gel containing ethidium bromide in Tris-acetate-EDTA (TAE) buffer [43].

The inhibitory effect of the two ZnO NPs on human topoisomerase I (Topo I) was also investigated by assessing their ability to relax supercoiled pBR322 plasmid DNA (100 µg) in the absence and presence of ZnO NP samples. They were used at concentrations ranging from 3% to 0.75% in 10× TGS buffer. Each reaction mixture was incubated at 37 °C for 1 hour. It was terminated by adding 4 µL of 5× loading buffer containing 4.5% sodium dodecyl sulfate (SDS), 0.25% bromophenol blue, and 45% glycerol. Electrophoresis was then performed on 1% agarose gels in 1× TAE buffer at 80 V for 60 minutes [44].

4. Results and Discussion

4.1. SEM and XRD Analysis Results of Apple (S1), Linden (S2) Samples

Figure 2(a) shows that zinc oxide nanoparticles (ZnO NPs) synthesized using apple extract consist of porous structures. At higher magnification (Figure 2(b)), these structures were observed to be composed of dot-shaped ZnO particles with sizes ranging from 10 to 30 nm. Figures 2(c–d) present ZnO NPs produced from linden extract; in the scanning electron microscopy (SEM) images, red blood cell-like ZnO nanostructures were detected. At higher magnification (Figure 2(d)), these nanostructures were further resolved as dot-shaped ZnO particles with dimensions of 10–20 nm.

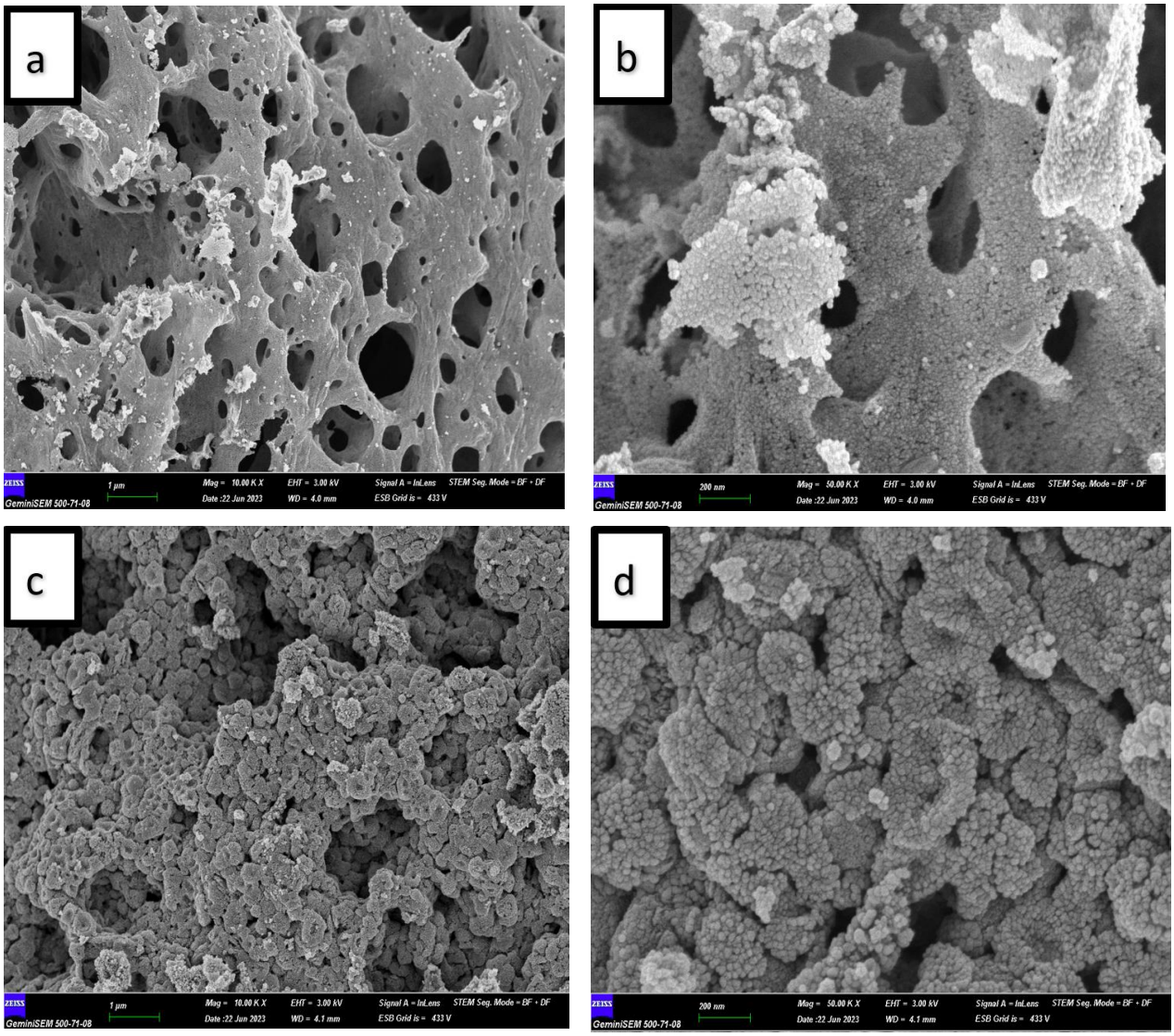


Figure 2. SEM images of ZnO NP's produced from **(a)-(b)** apple (S1) and **(c)-(d)** linden (S2) extract; Photographs at **(a)-(c)** 10,000, and **(b)-(d)** 50,000 times magnification

Similar dot-shaped ZnO nanostructures of varying sizes have been reported in several studies. For example, Joulaee et al. [45] synthesized ZnO nanoparticles (NPs), nickel oxide nanoparticles (NiO NPs), ZnO/NiO nanocomposites (NCs), and ZnO/NiO/graphene quantum dot nanocomposites (ZnO/NiO/GQDs NCs) via a novel green co-deposition and hydrothermal approach, reporting ZnO dots with diameters of 74 nm. Tshangana et al. [46] investigated the photocatalytic and antimicrobial activities of ZnO nanohybrids (ZnO-NFs@GQDs and ZnO-NRs@GQDs) and determined the average ZnO dot radius to be 23.5 nm. Similarly, Camacho et al. [47] synthesized ZnO nanoparticles using Ipomoea stans leaf extracts. Their characterization confirmed the presence of active functional groups and Zn–O bonds, while photocatalytic tests demonstrated more than 91% degradation efficiency against methyl orange, methylene blue, and rhodamine B dyes, with particle sizes ranging from 10.16 to 30.78 nm.

X-ray diffraction analysis revealed diffraction peaks at 2θ = 31.90°, 34.57°, 36.41°, 47.70°, 56.76°, 62.97°, 66.58°, 68.07°, 69.21°, 72.75°, 76.98°, and 81.51°, which correspond to the (100), (002), (101), (102), (110), (103), (200), (112), (201), (004), (202) and (104) planes, respectively. These reflections are characteristic of the wurtzite (hexagonal) crystal structure of ZnO. Furthermore, the XRD pattern shown in Figure 3 indicates the absence of any impurity or secondary diffraction peaks, confirming the purity of the hexagonal ZnO structure. The obtained diffraction peaks are in good agreement with previously reported studies [48,49].

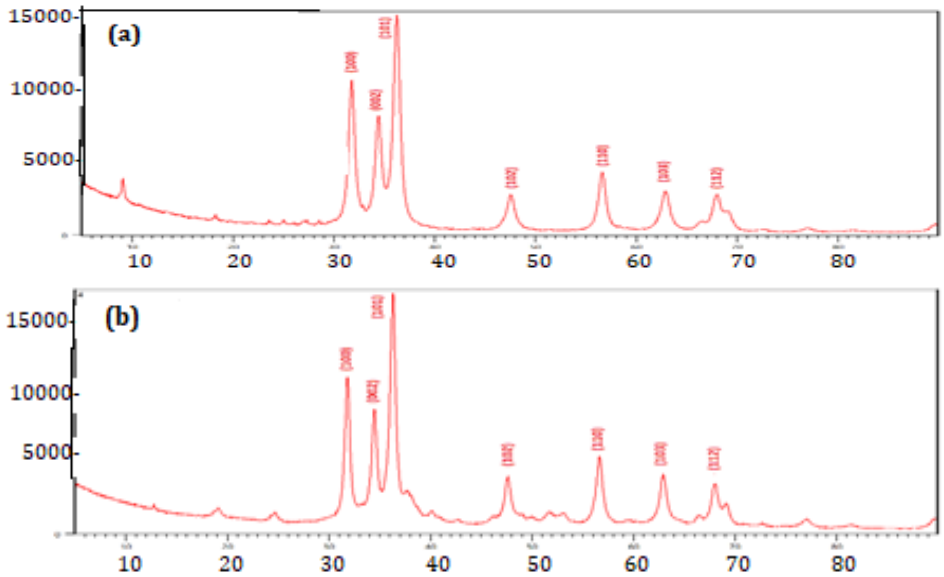


Figure 3. XRD analysis results of ZnO NPs produced from plant extract: **(a)** apple (S1), and **(b)** linden (S2)

The average crystallite size of the ZnO NP samples was estimated using the Debye–Scherrer equation:

$$D = \frac{K\lambda}{\beta Cos\theta} \tag{4.1}$$

From (4.1), D represents the average crystallite size, K is the Scherrer constant (≈0.9), λ is the wavelength of the X-rays (CuKα, 1.542 Å), β is the full width at half maximum (FWHM) of the diffraction peak, and θ is the Bragg diffraction angle. Based on this calculation, the average crystallite sizes of the ZnO NPs were determined to be 27 nm for the apple extract and 36 nm for the linden extract. These values are consistent with those reported for ZnO NPs synthesized from Hibiscus, Azolla, and Ipomoea leaf extracts [6,7,47].

4.2. FTIR Analysis Results of Apple (S1), Linden (S2) Samples

Fourier Transform Infrared Spectroscopy was employed to analyze the chemical structures of the synthesized ZnO nanoparticles. The positions of the absorption bands and the number of peaks observed are influenced by the crystal structure, type of chemical bonding, and morphology of the material. The characteristic FTIR peaks and corresponding band assignments of ZnO NPs are presented in Table 2 and Figure 4, respectively.

Table 2. FTIR band analysis results of ZnO NPs from plants

Peaks	ZnO (cm^{-1})	Assignments	References
1	526.96–551.04	Stretching of (Zn–O) bond	[17], [19]
2	813.74	C–H vibration	[18], [20]
3	1067.0–1069.1	C–H vibration; C–O stretching	[18]
4	1322.4–1376.6	C–H vibration	[18]
5	1661.4	C=O stretching vibration	
6	2142.2	C=O stretching	[18]
7	2353.4–2357.8	C=O stretching	[18]
8	2918.1	C–H stretching vibration	[18], [20]

A broad absorption band observed in the range of 2700–3500 cm-¹, together with a peak at 1092 cm-¹, corresponds to the O–H stretching vibration of polymeric H2O molecules associated with the Zn–O lattice. The absorption peak between 2344 and 2352 cm-¹ is attributed to atmospheric CO2. Since measurements were conducted at room temperature under ambient air conditions, contributions from moisture (H2O) and CO2 absorption were unavoidable. Notably, the absence of peaks just above 3000 cm-¹ indicates that the S1 and S2 samples do not contain aromatic flavonoid or phenolic chromophore structures.

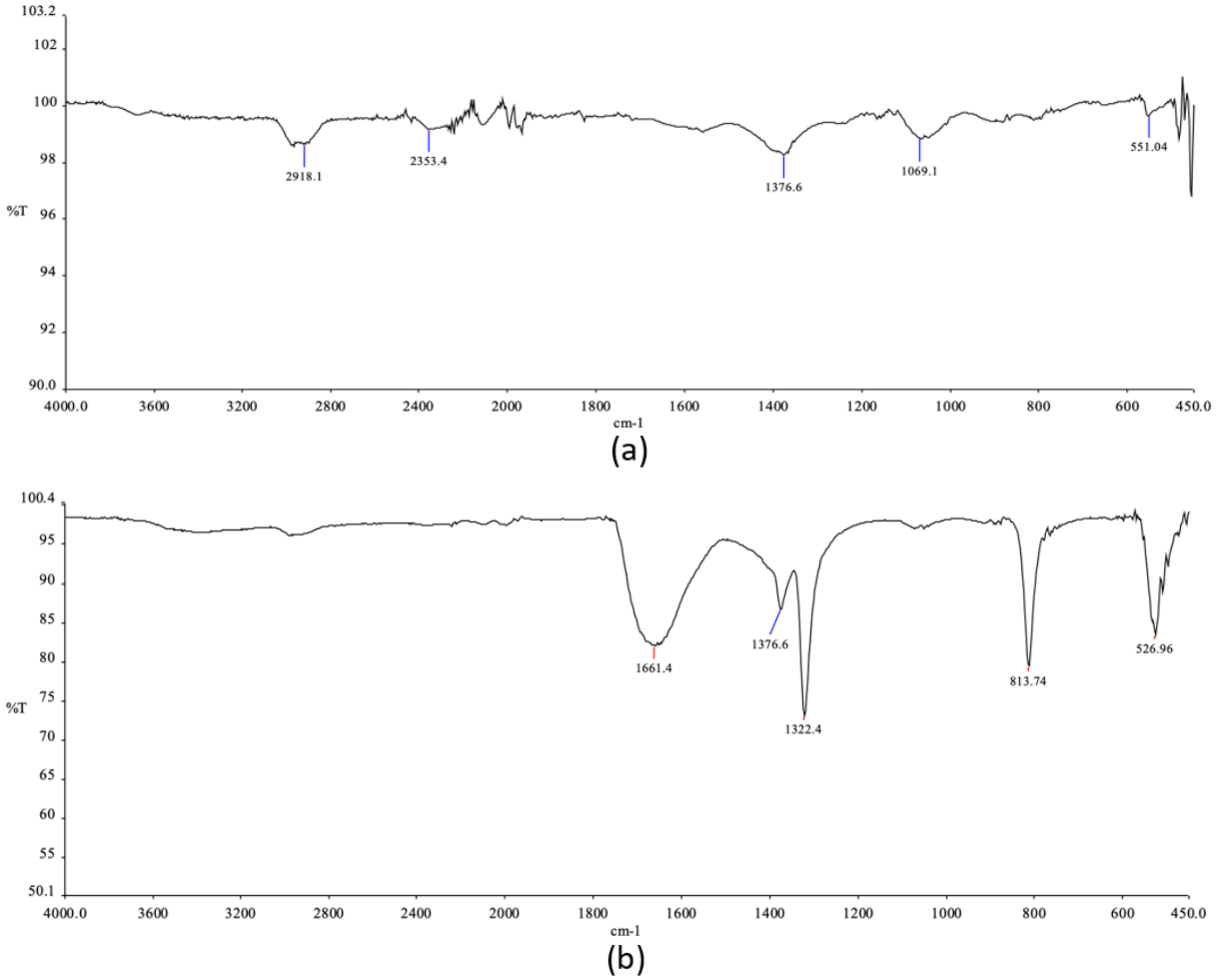


Figure 4. FTIR analysis results of ZnO NPs produced from plant extract: **(a)** apple (S1), and **(b)** linden (S2)

4.3. Samples CT-DNA Binding Experiment of Apple (S1), Linden (S2) Samples

The binding interactions of zinc oxide nanoparticles from two plants with calf thymus DNA (CT-DNA) were evaluated by agarose gel electrophoresis. Results are presented in Figure 5. In this assay, the concentrations of all nanoparticle samples were fixed at 100 μM, while the CT-DNA concentration was gradually decreased from 2 mg/mL to 1 mg/mL.

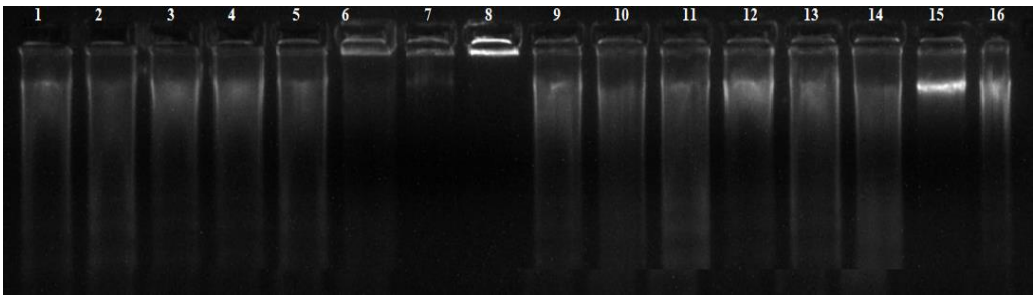
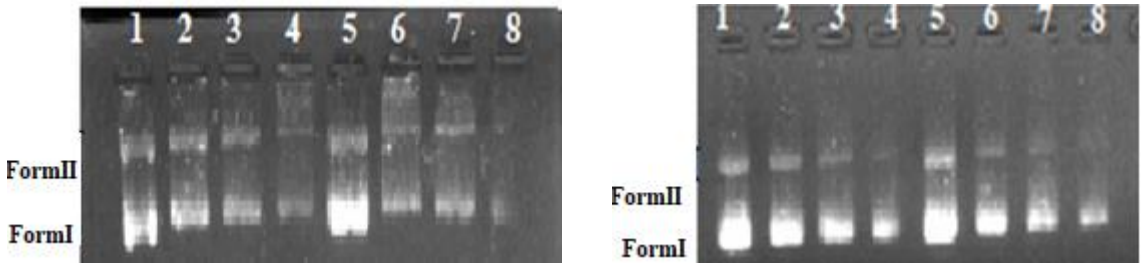


Figure 5. Agarose gel electrophoresis of S1, S2 samples. Ingredients of lines. Line1,5, 9,13: CT-DNA (2mg/mL) in buffer (pH=7), Line2-4: CT-DNA (2-0.5mg/mL) +buffer+sample S1 (%3), Line 14-16: CT-DNA (2-0.5mg/mL)+ buffer+sample S2 (%3)

The electrophoretic bands were assessed relative to the brightness and quenching of the control lanes containing CT-DNA alone (lanes 1, 5, 9, and 13). No DNA binding or interaction was observed at any concentration for sample S1. In contrast, sample S2 exhibited interaction with CT-DNA at the concentration of 1 mg/mL, indicating partial binding under these conditions.

4.4. Result of the DNA Cleavage Experiment of Apple (S1), Linden (S2) Samples

As shown in Figure 6(a–b), partial DNA cleavage was observed in lanes 1 and 5, which was attributed to the effect of water on pBR322 DNA. In the remaining lanes containing the nanoparticle samples, a reduction in the degree of DNA separation was detected. Since this phenomenon was observed in both samples, the overall DNA cleavage activity of the ZnO NPs was determined to be weak.



(a) **(b)**

Figure 6. Agarose gel electrophoresis of S1, S2 samples. Ingredients of lines **(a)**: Line1,5: pBR322DNA in dw, Line2-4: pBR322DNA in dw+ sample S1 (%3-%0.75), **(b)** Line1,5: pBR322DNA in dw, Line6-8: pBR322DNA in dw+ sample S2 (%3-%0.75)

4.5. Result of Human Topoisomerase -I Experiment of Apple (S1), Linden (S2) Samples

As shown in Figure 7, lane 1 demonstrates that the topoisomerase enzyme is active, as it successfully relaxes supercoiled DNA. In contrast, lane 5, containing irinotecan as a positive control, shows no relaxation, thereby confirming its inhibitory effect. In lanes 6 and 7, corresponding to sample S1, the inhibition of topoisomerase activity is evident, as DNA relaxation and the formation of Form II are prevented. Conversely, in lanes 12 and 13, partial DNA relaxation is observed for sample S2, indicating that it does not exhibit strong inhibitory activity. These results suggest that only sample S1 has the potential to act as an effective human topoisomerase I inhibitor, while sample S2 does not demonstrate significant inhibitory properties.

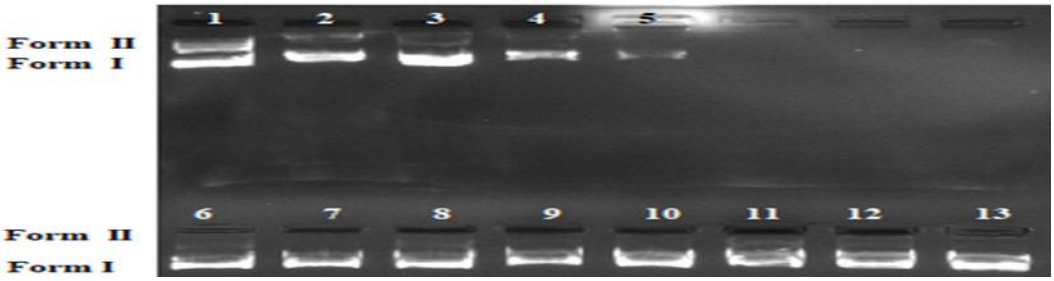


Figure 7. The inhibitory effects against the S1 and S2 samples. Lane 1: pBR322DNA +1 Unit Topo-I; Lane 2: pBR322DNA in buffer (TGS); Lane 3: pBR322DNA st human topoisomerase I of Control; Lane 4: pBR322DNA + 1 Unit Topo I + buffer (TGS); Lane 5: pBR322DNA + 1 Unit Topo I + buffer (TGS)+ irinotecan (3%); Line 6-7: pBR322DNA + 1 Unit Topo I + buffer (TGS)+ S1 (3-1.5%); Lane 12-13: pBR322DNA + 1 Unit Topo I + buffer (TGS)+ S2 (3-1.5%)

4.6. Antimicrobial Activity Results of Apple (S1), Linden (S2) Samples

4.6.1. Agar Diffusion Method

Zinc oxide nanoparticles synthesized from the extracts of two plant sources were dissolved in dimethylformamide (DMF). Their antimicrobial activity was evaluated against two kinds of Gram-positive bacteria, such as Staphylococcus epidermidis ATCC 12228, Bacillus cereus NRRL B-3008, and two kinds of

Gram-negative bacteria, such as Escherichia coli ATCC 25922 and Klebsiella pneumoniae ATCC 13883. Antimicrobial effects were assessed using the agar well diffusion method at a concentration of 100 ppm.

The results demonstrated that ZnO NPs (S1 and S2), synthesized by the green synthesis (biomethod) from apple and linden extracts, had inhibitory activity against all four bacterial strains. Detailed results of the inhibition zone diameters are presented in Table 3.

Table 3. Antimicrobial effects of ZnO NPs synthesized from different plants

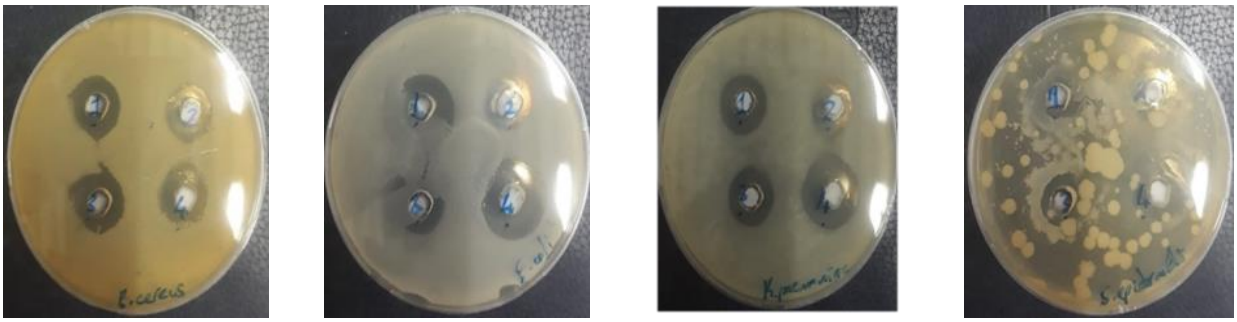
Microorganisms	S1 Sample	S2 Sample
Bacillus cereus	18mm	16mm
Escherichia coli	17mm	20mm
Klebsiella pneumonia	16mm	21mm
Staphylococcus epidermidis	12mm	16mm

**The inhibition zones include a hole diameter of 6 mm*

It was observed that the ZnO NPs synthesized from linden extract (Sample S2) exhibited the strongest antimicrobial effect, with the largest inhibition zone diameter (21 mm) recorded against *Klebsiella pneumoniae.*

4.6.2. Images of Individual Inhibition Zones of Samples in a Petri Dish

These findings indicate that the antimicrobial activity of zinc oxide nanoparticles (ZnO NPs) synthesized from different plant sources varies in effectiveness against different microorganisms. The corresponding results are presented in Figure 8(a–d).



(a) **(b)** **(c)** **(d)**

Figure 8. Observation of the antimicrobial effect of ZnO NPs obtained from two different plant samples (S1, S2 in well 2,3) on **(a)** *B. cereus*, **(b)** *E. coli*, **(c)** *K. pneumonia*, **(d)** *S. epidermidis*

For *Bacillus cereus*, the inhibition zone decreased from 18 mm in sample S1 to 16 mm in sample S2, suggesting a slight reduction in antimicrobial activity of the ZnO NPs synthesized from linden compared to those from apple. In the case of *Escherichia coli*, the inhibition zone increased from 17 mm in S1 to 20 mm in S2, indicating that the ZnO NPs derived from linden extract exhibited stronger antimicrobial activity against *E. coli* than those obtained from apple extract. For *Klebsiella pneumoniae*, the inhibition zone expanded markedly from 16 mm in S1 to 21 mm in S2, demonstrating a significant enhancement of antimicrobial efficacy in the linden-derived ZnO NPs. Similarly, against *Staphylococcus epidermidis*, the inhibition zone increased from 12 mm in S1 to 16 mm in S2, suggesting improved antimicrobial activity of the linden-derived ZnO NPs compared to the apple-derived counterparts.

Overall, these findings suggest that zinc oxide nanoparticles synthesized from different plant sources. Those derived from linden extract (Sample S2) generally exhibit stronger antimicrobial activity against the tested microorganisms compared to the apple-derived sample (S1). However, the extent of this enhancement varies depending on the specific microorganism.

The investigation of the antimicrobial effects of zinc oxide nanoparticles synthesized from different plant sources has produced noteworthy findings. The comparison between the two samples, S1 and S2, offers valuable insights into the influence of plant-derived precursors on the antimicrobial efficacy of ZnO NPs. Variations in inhibition zone sizes clearly indicate differences in biological activity depending on the source of synthesis. For example, *Bacillus cereus* exhibited a reduction in inhibition zone size from 18 mm in S1 to 16 mm in S2, suggesting a slight decrease in effectiveness when the NPs were synthesized from linden extract. In contrast, both *Escherichia coli* and *Klebsiella pneumoniae* displayed significant increases in inhibition zone diameters in S2 compared to S1, indicating enhanced antimicrobial activity of linden-derived ZnO NPs. Similarly, *Staphylococcus epidermidis* showed an increase from 12 mm to 16 mm, suggesting improved efficacy against this Gram-positive bacterium in the S2 sample.

Collectively, these results demonstrate that the antimicrobial potential of ZnO NPs is influenced by the choice of plant extract used in green synthesis. While certain microorganisms exhibited reduced sensitivity, others showed markedly enhanced susceptibility, highlighting the importance of plant source selection in tailoring the biological activity of ZnO NPs.

The plants used in ZnO NP synthesis contain flavonoids and phytochemicals, most notably the yellow pigment quercetin. While pure ZnO is characteristically white, these phytochemicals impart a slightly yellow hue to the reaction mixture. Because the phytochemicals are present only in trace amounts, ZnO remains the dominant component. Importantly, it is nearly impossible to synthesize 100% pure nano-ZnO from different plant extracts, as the resulting product inevitably contains residual biomolecules from the extract. Consequently, the biological activity, such as antimicrobial efficacy, varies, as the final product is effectively a mixture named biomass.

The composition of the plant extract used for synthesis, therefore, plays a critical role, as it determines the nature of residual biomolecules that interact with bacteria. Variations in pH, organic constituents, and molecular structures across different plant sources influence these interactions, ultimately leading to differences in the antibacterial activity of ZnO NPs synthesized from apple (S1) and linden (S2) extracts.

5. Conclusion

In conclusion, it was not possible to obtain fully pure ZnO nanoparticles using the environmentally friendly, chemical-free green synthesis approach applied in this study. Instead, the process yielded a mixture of nano ZnO and biomass powder containing varying phytochemical components, depending on the plant source. This compositional variation accounts for the differences in the biological activities observed.

The biomass obtained from *Malus domestica* (apple) demonstrated topoisomerase inhibition, thereby suppressing replication enzyme activity and indicating its potential as an anticancer agent. In contrast, the biomass derived from linden exhibited notable interactions with DNA and bacteria, suggesting significant antibacterial activity and highlighting its potential as a therapeutic agent. Overall, the findings of this study contribute valuable insights into the development of novel antimicrobial agents and enzyme inhibitors, with promising applications in health and biotechnology.

Author Contributions

All the authors equally contributed to this work. They all read and approved the final version of the paper.

Conflict of Interest

All the authors declare no conflict of interest.

Ethical Review and Approval

No approval from the Board of Ethics is required.

Acknowledgment

XRD, SEM, and FTIR analyses in this study were carried out at the Erciyes University Technology Research Application Center. This study was supported by the project numbered TSA-2022-1066 submitted to the Kayseri University Scientific Research Projects Coordination Unit. We would like to thank the Proofreading & Editing Office of the Dean for Research at Erciyes University for the copy editing and proofreading service for this manuscript.

References

[1] H. Agarwal, S. Venkat Kumar, S. Rajeshkumar, *A review on green synthesis of zinc oxide nanoparticles – An eco-friendly approach*, Resource-Efficiency and Technologies 3 (4) (2017) 406–413.

[2] R. Prasad, A. Bhattacharyya, Q. D. Nguyen, *Nanotechnology in sustainable agriculture: Recent developments, challenges, and perspectives*, Frontiers in Microbiology 8 (2017) 1014.

[3] C. O. Dimkpa, P. S. Bindraban, *Fortification of micronutrients for efficient agronomic production: a review*, Journal of Agricultural and Food Chemistry 36 (2016) 7.

[4] G. Marslin, K. Siram, Q. Maqbool, R. K. Selvakesavan, D. Kruszka, P. Kachlicki, G. Franklin, *Secondary metabolites in the green synthesis of metallic nanoparticles*, Materials 11 (6) (2018) 940.

[5] S. Gunalan, R. Sivaraj, V. Rajendran, *Green synthesized ZnO nanoparticles against bacterial and fungal pathogens*, Progress in Natural Science: Materials International 22 (6) (2012) 693–700.

[6] N. Bala, S. Saha, M. Chakraborty, M. Maiti, S. Das, R. Basu, P. Nandy, *Green synthesis of zinc oxide nanoparticles using Hibiscus subdariffa leaf extract: effect of temperature on synthesis, anti-bacterial activity and anti-diabetic activity*, Royal Society of Chemistry Advances 5 (7) (2015) 4993-5003.

[7] A. A. Zahir, A. A. Rahuman, *Evaluation of different extracts and synthesised silver nanoparticles from leaves of Euphorbia prostrata against Haemaphysalis bispinosa and Hippobosca maculata*, Veterinary Parasitology 187 (3-4) (2012) 511–520.

[8] K. Gudikandula, S. Charya Maringanti, *Synthesis of silver nanoparticles by chemical and biological methods and their antimicrobial properties*, Journal of Experimental Nanoscience 11 (9) (2016) 714–721.

[9] S. Kunjiappan, R. Chowdhury, C. Bhattacharjee, *A green chemistry approach for the synthesis and characterization of bioactive gold nanoparticles using Azolla microphylla methanol extract*, Frontiers of Materials Science 8 (2014) 123–135.

[10] M. Gomathi, P. V. Rajkumar, A. Prakasam, K. Ravichandran, *Green synthesis of silver nanoparticles using Datura stramonium leaf extract and assessment of their antibacterial activity*, Resource Efficiency and Technologies 3 (2017) 280–284.

[11] G. Bagherzade, M. M. Tavakoli, M. H. Namae, *Green synthesis of silver nanoparticles using aqueous extract of saffron (Crocus sativus L.) wastages and its antibacterial activity against six bacteria*, Asian Pacific Journal of Tropical Biomedicine 7 (3) (2017) 227–233.

[12] M. Yasir, J. Singh, M. K. Tripathi, P. Singh, R. Shrivastava, *Green Synthesis of Silver Nanoparticles Using Leaf Extract of Common Arrowhead Houseplant and Its Anticandidal Activity*, Pharmacognosy Magazine 13 (Suppl 4) (2018) 840–844.

[13] S. Swain, S. K. Barik, T. Behera, S. K. Nayak, S. K. Sahoo, S. S. Mishra, P. Swain, *Green Synthesis of Gold Nanoparticles Using Root and Leaf Extracts of Vetiveria zizanioides and Cannabis sativa and its Antifungal Activities*, BioNanoScience 6 (2016) 205–213.

[14] B. Kumar, K. Smita, L. Cumbal, A. Debut, *Green synthesis of silver nanoparticles using Andean blackberry fruit extract*, Saudi Journal of Biological Sciences 24 (1) (2017) 45–50.

[15] N. Nazar, I. Bibi, S. Kamal, M. Iqbal, S. Nouren, K. Jilani, M. Umair, S. Ata, *Cu nanoparticles synthesis using biological molecule of P. granatum seeds extract as reducing and capping agent: Growth mechanism and photo-catalytic activity*, International Journal of Biological Macromolecules 106 (2018) 1203–1210.

[16] K. Cheirmadurai, S. R. Murali, P. Thanikaivelan, *Green synthesis of copper nanoparticles and conducting nanobiocomposites using plant and animal sources*, Royal Society of Chemistry Advances 4 (2014) 19507–19511.

[17] M. Nasrollahzadeh, S. Mohammad Sajadi, *Pd nanoparticles synthesized in situ with the use of Euphorbia granulate leaf extract: Catalytic properties of the resulting particles*, Journal of Colloid and Interface Science 462 (2016) 243–251.

[18] M. Nasrollahzadeh, S. M. Sajadi, M. Maham, *Green synthesis of palladium nanoparticles using Hippophae rhamnoides Linn leaf extract and their catalytic activity for the Suzuki–Miyaura coupling in water*, Journal of Molecular Catalysis A: Chemical 396 (2015) 297–303.

[19] B. Zheng, T. Kong, X. Jing, T. Odoom-Wubah, X. Li, D. Sun, F. Lu, Y. Zheng, J. Huang, Q. Li, *Plant-mediated synthesis of platinum nanoparticles and its bioreductive mechanism*, Journal of Colloid and Interface Science 396 (2013) 138–145.

[20] D. Suresh, P.C. Nethravathi, Udayabhanu, H. Rajanaika, H. Nagabhushana, S. C. Sharma, *Green synthesis of multifunctional zinc oxide (ZnO) nanoparticles using Cassia fistula plant extract and their photodegradative, antioxidant and antibacterial activities*, Materials Science in Semiconductor Processing 31 (2015) 446–454.

[21] K. Elumalai, S. Velmurugan, *Green synthesis, characterization, and antimicrobial activity of zinc oxide nanoparticles from the leaf extract of Azadirachta indica (L.)*, Applied Surface Science 345 (2015) 329–336.

[22] R. Dobrucka, J. Dlugaszewska, *Biosynthesis and antibacterial activity of ZnO nanoparticles using Trifolium pratense flower extract*, Saudi Journal of Biological Sciences 23 (4) (2016) 517–523.

[23] M. Anbuvannan, M. Ramesh, G. Viruthagiri, N. Shanmugam, N. Kannadasan, *Anisochilus carnosus leaf extract mediated synthesis of zinc oxide nanoparticles for antibacterial and photocatalytic activities*, Materials Science in Semiconductor Processing 39 (2015) 621–628.

[24] P. C. Nagajyothi, T. V. M. Sreekanth, C. O. Tettey, Y. I. Jun, S. H. Mook, *Characterization, antibacterial, antioxidant, and cytotoxic activities of ZnO nanoparticles using Coptidis Rhizoma*, Bioorganic & Medicinal Chemistry Letters 24 (17) (2014) 4298–4303.

[25] V. V. Gawade, N. L. Gavade, H. M. Shinde, S. B. Babar, A. N. Kadam, K. M. Garadkar, *Green synthesis of ZnO nanoparticles by using Calotropis procera leaves for the photodegradation of methyl orange*, Journal of Materials Science: Materials in Electronics 28 (2017) 14033–14039.

[26] P. Rajiv, S. Rajeshwari, R. Venckatesh, Bio-Fabrication of zinc oxide nanoparticles using leaf extract of Parthenium hysterophorus L. and its size-dependent antifungal activity against plant fungal pathogens, Spectrochimica Acta Part A: Molecular and Biomolecular Spectroscopy 112 (2013) 384–387.

[27] A. Raza, X. Xu, L. Xia, C. Xia, J. Tang, Z. Ouyang, *Quercetin-iron complex: synthesis, characterization, antioxidant, DNA binding, DNA cleavage, and antibacterial activity studies*, Journal of Fluorescence 26 (2016) 2023–2031.

[28] M. Tan, J. Zhu, Y. Pan, Z. Chen, H. Liang, H. Liu, H. Wang, *Synthesis, Cytotoxic Activity, and DNA Binding Properties of Copper (II) Complexes with Hesperetin*, Naringenin, and Apigenin, Bioinorganic Chemistry and Applications 2009 (1) (2009) 347872.

[29] G. Marslin, R. K. Selvakesavan, G. Franklin, B. Sarmento, A. C. P. Dias, *Antimicrobial activity of cream incorporated with silver nanoparticles biosynthesized from Withania somnifera*, International Journal of Nanomedicine 10 (1) (2015) 5955–5963.

[30] S. Jain, M. S. Mehata, *Medicinal Plant Leaf Extract and Pure Flavonoid Mediated Green Synthesis of Silver Nanoparticles and their Enhanced Antibacterial Property*, Scientific Reports 7 (2017) 15867.

[31] G. Krishnan, J. Subramaniyan, P. C. Subramani, B. Muralidharan, D. Thiruvengadam, *Hesperetin conjugated PEGylated gold nanoparticles exploring the potential role in anti-inflammation and anti-proliferation during diethylnitrosamine-induced hepatocarcinogenesis in rats*, Asian Journal of Pharmaceutical Sciences 12 (5) (2017) 442–455.

[32] B. Zhao, X. Cao, R. De La Torre-Roche, C. Tan, T. Yang, J. C. White, H. Xiao, B. Xing, L. He, *A green, facile, and rapid method for microextraction and Raman detection of titanium dioxide nanoparticles from milk powder*, Royal Society of Chemistry Advances 7 (35) (2017) 21380–21388.

[33] D. Xiao, C. Zhang, D. Yuan, J. He, J. Wu, K. Zhang, R. Lin, H. He, *Magnetic solid-phase extraction based on Fe3O4 nanoparticle retrieval of chitosan for the determination of flavonoids in biological samples coupled with high performance liquid chromatography*, Royal Society of Chemistry Advances 4 (110) (2014) 64843–64854.

[34] E. Abbasi, M. Milani, S. F. Aval, M. Kouhi, A. Akbarzadeh, H. T. Nasrabadi, P. Nikasa, S. W. Joo, Y. Hanifehpour, K. Nejati-Koshki, M. Samiei, *Silver nanoparticles: Synthesis methods, bio-applications and properties*, Critical Reviews in Microbiology 42 (2) (2016) 173–180.

[35] B. Kumar, K. Smita, L. Cumbal, A. Debut, *Green Approach for Fabrication and Applications of Zinc Oxide Nanoparticles*, Bioinorganic Chemistry and Applications 2014 (1) (2014) 523869.

[36] M. A. Hossain, S. Islam, *Synthesis of carbon nanoparticles from kerosene and their characterization by SEM/EDX, XRD and FTIR*, American Journal of Nanoscience and Nanotechnology 1(2) (2013) 52-56.

[37] M. N. S. Abdelaziz, M. G. Zayda, A. T. Maung, M. El-Telbany, T. N. Mohammadi, S. Z. C. Lwin, K. Z. Linn, C. Wang, L. Yuan, Y. Masuda, K. Honjoh, T. Miyamoto, *Genetic characterization, antibiotic resistance, and virulence genes profiling of Bacillus cereus strains from various foods in Japan*, Antibiotics 13(8) (2024) 774.

[38] S. Z. Öner, İ. Kaleli, M. Demir, A. Çalışkan, E. Mete, H. Şenol, *Gram-negative bacilli isolated from blood cultures and antimicrobial resistance*, Journal of the Turkish Microbiology Society 54(4) (2024) 274-281.

[39] R. Abbas, M. Chakkour, H. Z. E. Dine, E. F. Obaseki, S. T. Obeid, A. Jezzini, G. Ghssein, Z. Ezzeddine, *General overview of Klebsiella pneumonia: epidemiology and the role of siderophores in its pathogenicity*, Biology 13(2) (2024) 78.

[40] M. Moradinezhad, E. A. Montazeri, A. H. Ashtiani, R. Pourlotfi, V. Rakhshan, *Biofilm formation of Streptococcus mutans, Streptococcus sanguinis, Staphylococcus epidermidis, Staphylococcus aureus, Lactobacillus casei, and Candida Albicans on 5 thermoform and 3D printed orthodontic clear aligner and retainer materials at 3 time points: an in vitro study*, BMC Oral Health 24(1) (2024) 1107.

[41] A. M. Abu-Dief, R. M. El-Khatib, T. El-Dabea, M. Feizi-Dehnayebi, I. O. Barnawi, A. H. Alsehli, K. Al-Ghamdi, M. A. E. A. A. A. El-Remaily, *Design, preparation, physicochemical characterization, structural conformational, biological evaluation, and DNA interaction for some new benzimidazole complexes*, Applied Organometallic Chemistry 38(3) (2024) e7358.

[42] C. Perez, M. Pauli, P. Bazerque, *An antibiotic assay by the agar-well diffusion method*, Acta Biologica et Medica Experimentalis 15 (1990) 113–115.

[43] T. Keleş, B. Barut, A. Özel, Z. Bıyıklıoğlu, *Synthesis of water soluble silicon phthacyanine, naphthalocyanine bearing pyridine groups and investigation of their DNA interaction, topoisomerase inhibition, cytotoxic effects and cell cycle arrest properties*, Dyes and Pigments 164 (2019) 372–383.

[44] J. G. Deng, T. Li, G. Su, Q.-P. Qin, Y. Liu, Y. Gou, *Co(III) complexes based on α-N-heterocyclic thiosemicarbazone ligands: DNA binding, DNA cleavage, and topoisomerase I/II inhibitory activity studies*, Journal of Molecular Structure 1167 (2018) 33–43.

[45] S. Joulaee, M. Mirzaei, A. Hassanpour, H. Safardoust-Hojaghan, A. Khani, *Efficient removal of anionic and cationic dyes from waste water using green ZnO/NiO/graphene quantum dots nano photocatalyst*, Optik 290 (2023) 171324.

[46] C. Tshangana, M. Chabalala, A. Muleja, E. Nxumalo, B. Mamba, *Shape-dependant photocatalytic and antimicrobial activity of ZnO nanostructures when conjugated to graphene quantum dots*, Journal of Environmental Chemical Engineering 8 (4) (2020) 103930.

[47] D. Santana-Camacho, F. A. Barrios-Navarro, A. Moreno-Meza, A. Villegas-Fuentes, A. R. Vilchis-Nestor, P. A. Luque, *Photocatalytic properties of ZnO semiconductor nanoparticles green synthesized employing Ipomoea stans leave extracts*, Ceramics International: Part C 50 (21) (2024) 44426–44439.

[48] G. Marslin, R. K. Selvakesavan, G. Franklin, B. Sarmento, A. C. Dias, *Antimicrobial activity of cream incorporated with silver nanoparticles biosynthesized from Withania somnifera*, International Journal of Nanomedicine 10 (1) (2015) 5955–5963.

[49] S. Jain, M. S. Mehata, *Medicinal Plant Leaf Extract and Pure Flavonoid Mediated Green Synthesis of Silver Nanoparticles and their Enhanced Antibacterial Property*, Scientific Reports 7 (2017) 15867.